ChemComm
Chemical Communications

Accepted Manuscript

This article can be cited before page numbers have been issued, to do this please use: F. Towers Tompkins, L. Parker, R. Fogarty, J. Seymour, E. Gousseva, D. C. Grinter, R. Palgrave, C. D. Smith, R. Bennett, R. P. Matthews and K. R. J. Lovelock, *Chem. Commun.*, 2024, DOI: 10.1039/D4CC03388D.

ROYAL SOCIETY OF CHEMISTRY

rsc.li/chemcomm

ChemComm

View Article Online
DOI: 10.1039/D4CC03388D

COMMUNICATION

Controlling and Predicting Alkyl-Onium Electronic Structure

Frances K. Towers Tompkins,[a] Lewis G. Parker,[a] Richard M. Fogarty,[b] Jake M. Seymour,[a] Ekaterina Gousseva,[a] David C. Grinter,[c] Robert G. Palgrave,[d] Christopher D. Smith,[a] Roger A Bennett,[a] Richard P. Matthews,[e] Kevin R. J. Lovelock[a]

Received 00th January 20xx,
Accepted 00th January 20xx

DOI: 10.1039/x0xx00000x

X-ray photoelectron spectroscopy (XPS) and *ab initio* calculations show that fully alkylated onium cation electronic structure can be tuned using both the alkyl chains and the central onium atom. The key for tuning the central onium atom is methyl versus longer alkyl chains, allowing selection of the optimum cation for a wide range of applications, including catalysis and biocides.

Fully alkylated onium cations feature in a wide range of applications,[1] including organic synthesis,[2-4] biocides,[5, 6] electrochemical energy storage materials,[7, 8] friction/corrosion additives,[9, 10] and solar energy capture/storage materials[11]. Two key structural variations of alkylated oniums are: (i) the alkyl substituents, C_nH_{2n+1}, *e.g.* from four CH_3 in tetramethylammonium ($[N_{1,1,1,1}]^+$), to much longer alkyls; (ii) the central X atom *e.g.* tetraalkylammonium ($[N_{n,n,n,n}]^+$), trialkylsulfonium ($[S_{n,n,n}]^+$) or tetraalkylphosphonium ($[P_{n,n,n,n}]^+$) (Figure 1). This structural variation gives the potential to finely tune properties and performance,[8] although historically the focus has been on using the cation alkyl chain to control hydrophobicity or steric interactions.

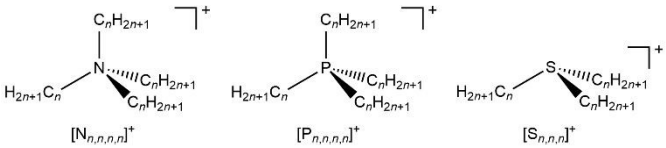

Figure 1. Fully alkylated onium cation structures (see ESI Section 3 for cations studied).

Electrostatic interactions are key for onium-anion and onium-neutral molecule interactions, as there are no π-bonds and only σ-bonds on fully alkylated onium cations. In synthesis, hydrogen bonding catalysis is based on electrostatic interactions between onium cations and substrates,[2, 3] and phase-transfer catalysis relies on anion-onium cation electrostatic interactions[4]. For biocides the first stage of $[N_{n,n,n,n}]^+$ interaction with a cell membrane is via an electrostatic interaction between the positively charged $[N_{n,n,n,n}]^+$ headgroup and anionic parts of the membrane.[5, 6, 12-15] Moreover, a single calculable electronic descriptor that can capture through-bond effects has been used to understand the impact of substituents on $[N_{n,n,n,n}]^+$,[16, 17] and a range of calculated electronic structure properties (*e.g.* orbital energies) have been used to predict the impact of $[N_{n,n,n,n}]^+$ supporting electrolytes on electrochemical performance[8]. Despite these extensive examples, there is still a large knowledge gap in the electronic structure of fully alkylated onium cations that underpins electrostatic interactions in the wide variety of applications. Using a combination of experimental X-ray photoelectron spectroscopy (XPS) and lone-ion-SMD (Solvation Model based on Density) density functional theory (DFT) calculations we provide both experimental and computational evidence on liquid-phase onium cations.

Element-specific XPS core-level binding energies, E_B(core), are capable of capturing multiple electronic structure descriptors for each onium cation, *e.g.* E_B(N 1s). Moreover, E_B(core) and the electrostatic potential at a nucleus, V_n, have been found to be linearly correlated for ionic liquids (ILs),[18, 19] meaning that E_B(core) can be readily interpreted unlike *e.g.* chemical shifts in NMR. Furthermore, V_n is an excellent localised non-covalent bonding/reactivity strength descriptor;[20] atoms with large E_B(core) and large V_n will attract electrons relative to atoms with small E_B(core) and small V_n.

ILs with relatively weakly interacting anions, *e.g.* $[NTf_2]^-$ (bis[(trifluoromethane)sulfonyl]imide) or $[FSI]^-$ (bis(fluorosulfonyl)imide), can be used to probe intrinsic cation properties, as cations are effectively in a sea of anions that give non-specific interactions.[18, 19] Additionally, lone-cation-SMD

[a] Department of Chemistry, University of Reading, UK
[b] Department of Chemistry, Imperial College London, UK
[c] Diamond Light Source, UK
[d] Department of Chemistry, University College London, UK
[e] Department of Biosciences, University of East London, UK
† k.r.j.lovelock@reading.ac.uk RMatthews3@uel.ac.uk
Electronic Supplementary Information (ESI) available: [details of any supplementary information available should be included here]. See DOI: 10.1039/x0xx00000x

calculations (*i.e.* with no counteranions) capture the inherent cation properties.

The range of onium cations studied in the liquid-phase using XPS to date is limited, with the main focus on onium cations in ILs[21-25] - which have sufficiently low vapour pressure to be used with standard XPS apparatus[26]. A key finding for XPS of $[N_{n,n,n,n}]^+$-based ILs was the impact of cations with linear (*e.g.* $[N_{6,6,6,14}]^+$ ammonium cation) versus ring (*e.g.* $[C_8C_1Pyrr]^+$ pyrrolidinium cation) alkyl on the IL electronic structure; cation-anion interactions were linked to the conformational flexibility of the cation.[22, 23] However, the number of different onium cations studied was relatively limited, leaving open questions, *e.g.* what is the influence of the alkyl substituent on onium electronic structure? Herein, we measured E_B(core) for 12 [onium cation][NTf_2] and two [onium cation][FSI] ILs using XPS and performed Ione-ion-SMD DFT calculations (ESI Section 3 for details) for 31 onium cations to address these questions.

Varying the alkyl chain length of $[N_{n,n,n,n}]^+$ from methyl to longer has a significant and predictable impact on $E_B(N_{cation}\ 1s)$. N 1s XPS for the two ILs $[N_{4,1,1,1}][NTf_2]$ and $[N_{4,2,2,2}][NTf_2]$ gave a relatively large $\Delta E_B(N_{cation}\ 1s)$ of -0.36 eV (Figure 2a, Figure 3a and ESI Table S8), representing $\Delta E_B(N_{cation}\ 1s)$ going from three CH_3 to three longer alkyl chains. Each successive change of one CH_3 to one longer alkyl gives $\Delta E_B(N_{cation}\ 1s)$ of ~-0.12 eV (Figure 2a), as demonstrated by $\Delta E_B(N_{cation}\ 1s)$ from $[N_{4,1,1,1}][NTf_2]$ to $[N_{3,2,1,1}][NTf_2]$ to $[N_{4,4,4,1}][NTf_2]$ to $[N_{4,2,2,2}][NTf_2]$ (Figure 2a, Figure 3a and ESI Table S8). This effect of the alkyl chain lengths on cation electronic structure is independent of the anion identity, as the same $\Delta E_B(N_{cation}\ 1s)$ effect is observed when the $[FSI]^-$ anion was used instead of $[NTf_2]^-$, *e.g.* $[N_{4,4,4,1}][FSI]$ versus $[N_{4,1,1,1}][FSI]$ (ESI Figure S17 and ESI Table S8).

Changing the alkyl substituent from ethyl to longer had no discernible impact on $E_B(N_{cation}\ 1s)$, with clear evidence from three cases: (i) $[N_{n,1,1,1}]^+$ (where n = 3, 4 and 6) gave the same $E_B(N_{cation}\ 1s)$; (ii) $[N_{n,2,2,2}]^+$ (where n = 4 and 8) gave the same $E_B(N_{cation}\ 1s)$; (iii) $[N_{4,4,4,1}]^+$ and $[N_{8,8,8,1}]^+$ gave the same $E_B(N_{cation}\ 1s)$ (Figure 2a and ESI Table S8).

Linear versus large ring alkyl chains, *e.g.* ammonium versus pyrrolidinium, had no discernible impact on experimental $E_B(N_{cation}\ 1s)$. Cations with one CH_3 substituent and either all linear longer alkyl chains ($[N_{4,4,4,1}][NTf_2]$, $[N_{8,8,8,1}][NTf_2]$) or large ring alkyl chains ($[C_4C_1Pip][NTf_2]$, $[C_8C_1Pyrr][NTf_2]$) gave the same $E_B(N_{cation}\ 1s)$ within experimental uncertainty (Figure 2a and ESI Table S8).

Calculated $E_B(N_{cation}\ 1s)$ match the experimental $E_B(N_{cation}\ 1s)$ very well, both visually (Figure 2a, Figure 2b and ESI Figure S18), and an excellent linear correlation for calculated versus experimental $E_B(N_{cation}\ 1s)$ (ESI Figure S20). Going from $[N_{1,1,1,1}]^+$ to $[N_{2,2,2,2}]^+$, each time a CH_3 is changed to a longer alkyl chain gives $\Delta E_B(N_{cation}\ 1s)$ ~-0.08 eV (Figure 2b and Figure 3a), which is slightly smaller than the experimental $\Delta E_B(N_{cation}\ 1s)$ of ~-0.12 eV. This difference may arise from the choice of functional/basis set combinations; the wB97XD functional was selected as it has minimal self-interaction error and correctly describes long-range electron-electron interactions (important in determining ionisation energies). An alternative explanation is the failure of the SMD model to capture local interactions (switching from IL

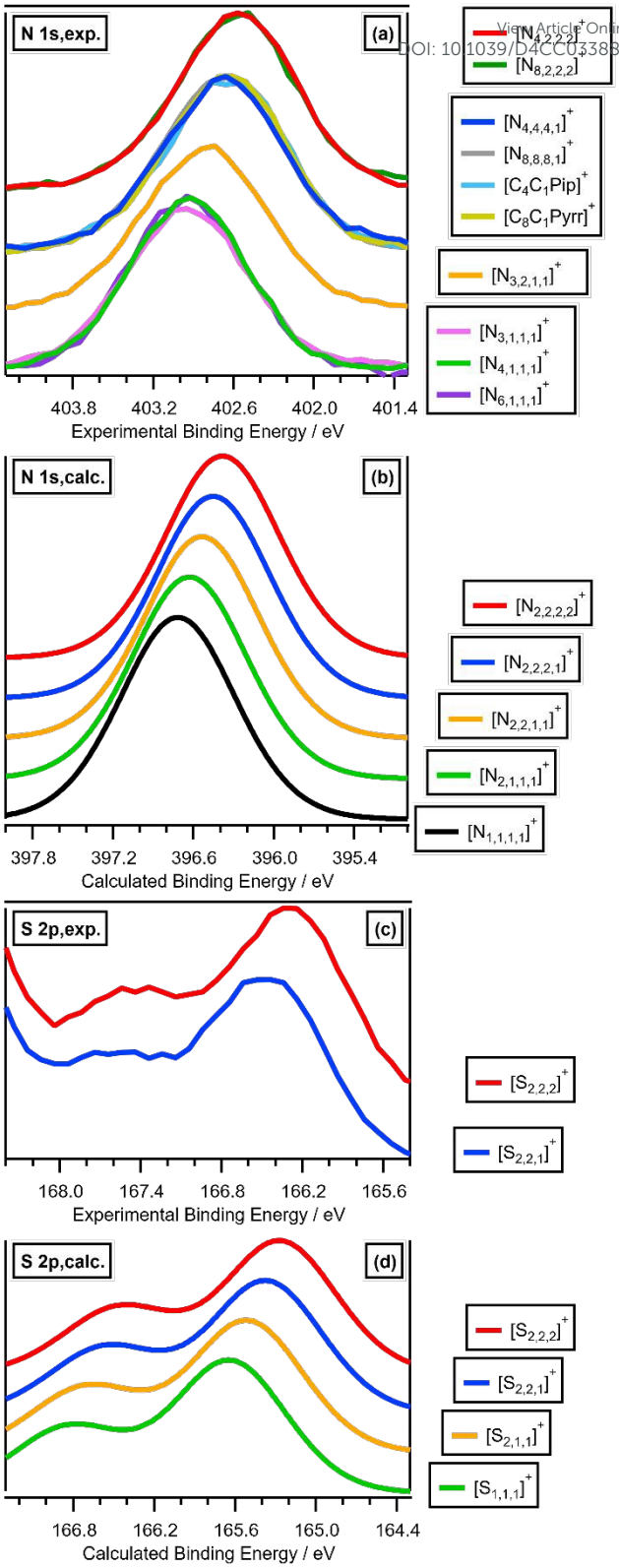

Figure 2. Experimental and calculated core XP spectra: (a) N 1s,exp. for [cation][NTf_2] where cation = $[N_{3,1,1,1}]^+$, $[N_{4,1,1,1}]^+$, $[N_{6,1,1,1}]^+$, $[N_{3,2,1,1}]^+$, $[N_{4,4,4,1}]^+$, $[N_{8,8,8,1}]^+$, $[C_4C_1Pip]^+$, $[C_8C_1Pyrr]^+$, $[N_{4,2,2,2}]^+$ and $[N_{8,2,2,2}]^+$; (b) N 1s,calc. for $[N_{1,1,1,1}]^+$, $[N_{2,1,1,1}]^+$, $[N_{2,2,1,1}]^+$, $[N_{2,2,2,1}]^+$ and $[N_{2,2,2,2}]^+$; (c) S 2p,exp. for $[S_{2,2,1}][NTf_2]$ and $[S_{2,2,2}][NTf_2]$; (d) S 2p,calc. for $[S_{1,1,1}]^+$, $[S_{2,1,1}]^+$, $[S_{2,2,1}]^+$ and $[S_{2,2,2}]^+$. Experimental XP spectra are area normalised and charge referenced using methods given in ESI Section 5. Traces are vertically offset for clarity.

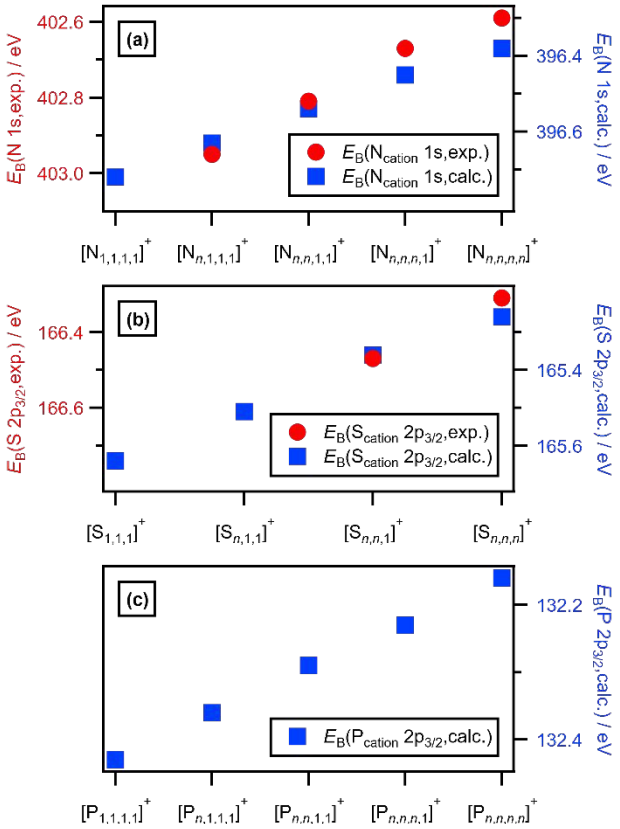

Figure 3. (a) Experimental and calculated E_B(N$_{cation}$ 1s). (b) Experimental and calculated E_B(S$_{cation}$ 2p$_{3/2}$). (c) Calculated E_B(P$_{cation}$ 2p$_{3/2}$). Where *n* is used as a label, $n \geq 2$.

SMD to water SMD had a small impact on ΔE_B(N$_{cation}$ 1s), Figures S19c and 19d and Table S9).

The effect of varying alkyl chain lengths for all key fully alkylated oniums is the same. For [S$_{n,n,n}$]$^+$ and [P$_{n,n,n,n}$]$^+$ cations the effect of changing from methyl to longer alkyl substituents on E_B(S$_{cation}$ 2p) and E_B(P$_{cation}$ 2p) respectively match those of E_B(N$_{cation}$ 1s) for [N$_{n,n,n,n}$]$^+$. Comparing experimental S 2p XPS for the two ILs [S$_{2,2,1}$][NTf$_2$] and [S$_{2,2,2}$][NTf$_2$] gave ΔE_B(S 2p$_{3/2}$) = -0.16 eV (Figure 2c and Figure 3b). Furthermore, going from [S$_{2,2,1}$]$^+$ to [S$_{2,2,2}$]$^+$, gives a calculated ΔE_B(S 2p$_{3/2}$) = -0.10 eV (Figure 2c, Figure 3b and ESI Table S8), demonstrating that the calculations match the experiments very well. Moreover, for [P$_{n,n,n,n}$]$^+$ each time a methyl is changed to a longer alkyl gives ΔE_B(P$_{cation}$ 2p$_{3/2}$) ~-0.07 eV (Figure 3c and ESI Figure S21).

The excellent matches for the experimental and calculated E_B(X$_{cation}$ core) (where X = N, S or P) demonstrate that the changes in the experimental E_B(X$_{cation}$ core) are due to ground state effects and can be related directly to the molecular electrostatic potential at the central onium atom nucleus, V_X (Figure 5). The differences in E_B(X$_{cation}$ core) for fully alkylated onium cations are explained by the alkyl group inductive effect, where the additive strength is -$CH_2CH_2CH_3$ ≈ -C_2H_5 < -CH_3.[27] Four CH_3 substituents gives the largest E_B(X$_{cation}$ core) = largest V_X = strongest X atom electrostatic interaction. Conversely, four longer alkyl substituents gives the smallest E_B(Ncation 1s) = smallest V_X = weakest X atom electrostatic interaction.

Changing the alkyl groups from linear to branched (*i.e.* going from each α-C atom having one C and two H to each α-C atom

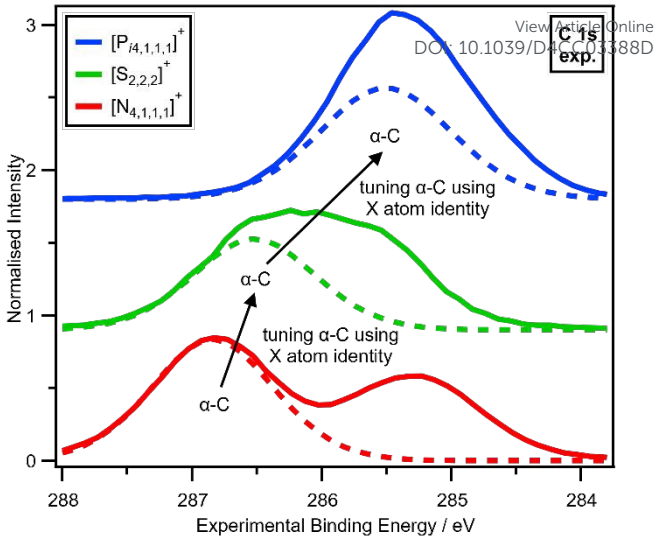

Figure 4. Tuning α-C using X atom identity. Experimental C 1s XP spectra for [P$_{i4,1,1,1}$][NTf$_2$], [S$_{2,2,2}$][NTf$_2$] and [N$_{4,1,1,1}$][NTf$_2$] ionic liquids. Experimental XP spectra are area normalised and charge referenced using methods given in ESI Section 5. Traces are vertically offset for clarity.

having two C and one H) gives a small impact on E_B(N$_{cation}$ 1s) and V_N. Changing the cation from [N$_{2,2,2,2}$]$^+$ to [N$_{i3,i3,i3,i3}$]$^+$ (*i*3 = isopropyl, ESI Table S3) gave ΔE_B(N$_{cation}$ 1s) = -0.09 eV (ESI Figure S22 and ESI Table S9). [N$_{i3,i3,i3,i3}$]$^+$ is unlikely to be stable in solution, but adding one branched alkyl group to give *e.g.* [N$_{i3,2,2,2}$]$^+$ will give stable cations and will allow small fine tuning of E_B(N$_{cation}$ 1s) and V_N.

The electronic environment of the carbon atoms in onium cations can be finely controlled by changing X$_{cation}$ (Figure 4 and ESI Section 14), as demonstrated by using our second spectroscopic handle, E_B(C 1s). E_B(C$_{α-C}$ 1s) and therefore V_C can be tuned using the central X atom identity. The experimental order for E_B(C$_{α-C}$ 1s) is N > S > P (Figure 4 upper), which matches literature E_B for N versus P (S was not included in that publication) and also partial charge calculations.[22, 28] E_B(C$_{α-C}$ 1s) following N > S > P matches the order of the central atom electronegativity, *i.e.* N > S > P, so nitrogen withdraws the most electron density from α-C to X$_{cation}$ (Figure 5).

V_X for X$_{cation}$ can be inferred from E_B(C$_{α-C}$ 1s), given that all onium cations will have approximately the same overall charge of +1, so any change in $V_{α-C}$ will have the opposite effect on V_X. E_B(C$_{α-C}$ 1s) and $V_{α-C}$ trend N > S > P, so V_X (relative to a neutral X

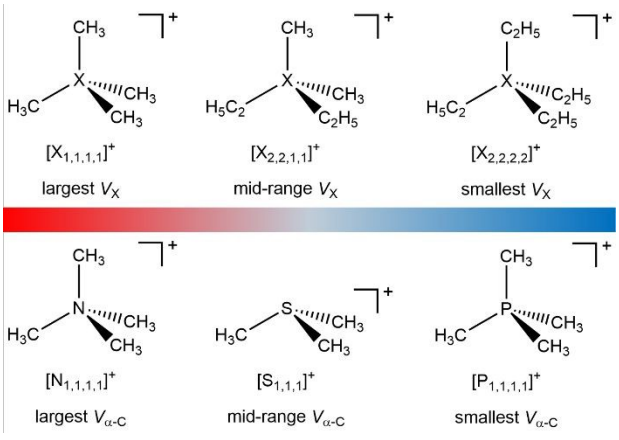

Figure 5. Effect of the onium cation structure on V_X and $V_{α-C}$.

atom) trends P > S > N.

Both $E_B(X_{cation}$ core) and $E_B(C_{\alpha\text{-}C}$ 1s) can be tuned using the counteranion identity.[19, 21, 22] Changing from Cl^- to $[NTf_2]^-$ had the same effect (within experimental uncertainty) of +0.4 eV on $E_B(C_{\alpha\text{-}C}$ 1s), $\Delta E_B(N_{cation}$ 1s) and $\Delta E_B(P_{cation}$ 2p).[19, 21, 22] This effect of the anion is similar in magnitude to changing from four alkyl substituents to four longer alkyl substituents (Figure 3).

Given that the onium cation headgroup will dominate any electrostatic interaction with a substrate, both V_X and $V_{\alpha\text{-}C}$ are clearly vital descriptors. We have demonstrated that both V_X and $V_{\alpha\text{-}C}$ can be predictably controlled for onium cations by the choice of alkyl chain length and central X atom identity. Furthermore, for certain applications where cation-anion are likely to be bound together (*e.g*. ion pairing in solvents with low relative permittivity, in ionic liquids), the counteranion identity can also contribute strongly to both V_X and $V_{\alpha\text{-}C}$.

We envisage this information being useful in two areas. Firstly, V_X and $V_{\alpha\text{-}C}$ are expected to be very useful descriptors for developing models using both quantitative structure-property relationships (QSPR) and machine learning. Such descriptors could be calculated using the same DFT methods demonstrated here, or a cheaper but cruder method would be to use the linear relationships developed here to make predictions of V_X and $V_{\alpha\text{-}C}$. Secondly, a semi-quantitative judgement of the optimum onium cation to be used in any application can be made using our results. The largest V_X (*i.e*. strongest X atom electrostatic interaction) would be $[X_{1,1,1,1}][FAP]$ (the very weakly electrostatically interacting anion $[FAP]^-$ = tris(pentafluoroethyl)trifluorophosphate[19]), and the smallest V_X (*i.e*. weakest X atom electrostatic interaction) would be *e.g*. $[X_{2,2,2,2}]Cl$. For biocides for example, a strong electrostatic interaction is expected to be desirable. Therefore, focusing on electronic effects (and ignoring steric effects) $[X_{1,1,1,1}]^+$ would be better than $[X_{2,2,2,2}]^+$. However, such a selection is challenging as both V_X and $V_{\alpha\text{-}C}$ are affected in opposite directions by the central X atom identity, and a single site interaction model cannot be assumed. Essentially, the electrostatic interactions are too complicated for a single metric to be used for judgement.

Overall, we have presented new experimental and calculated electronic descriptors for judging electrostatic interaction strengths in fully-alkylated onium cations (Figure 5). X_{cation}, α-C and C_{alkyl} can be predictably tuned using a combination of the alkyl chain lengths, the central X atom identity and the counteranion. In future work we will aim to demonstrate further control onium electronic structure using heteroatom substituents (*e.g*. O atoms) or X-H (protic cations).

Data Availability Statement

The data underlying this study are openly available in the University of Reading Research Data Archive at [DOI to be added once obtained]

Conflicts of interest

There are no conflicts to declare.

Notes and references

View Article Online
DOI: 10.1039/D4CC03388D

‡ KRJL acknowledges support from a Royal Society University Research Fellowship (URF\R\150353 and URF\R\211005). JMS acknowledges support from a Royal Society University Research Fellowship Enhancement Award (RGF\EA\180089). EG acknowledges support from a Royal Society Research Grant for Research Fellows (RGF\R1\180053). LGP and FKTT acknowledge support from Royal Society Research Fellows Enhanced Research Expenses (RF\ERE\210061 and RF\ERE\231015). RPM acknowledges support from the Royal Society of Chemistry through the RSC Research Fund grant (R21-4762139998). We acknowledge Diamond Light Source for time on Beamline B07-B under Proposals SI29413, SI30367, SI31939, SI33378 and SI35207.

1. F. Bures, *Top. Curr. Chem.*, 2019, **377**, 14.
2. S. Shirakawa, S. Y. Liu, S. Kaneko, Y. Kumatabara, A. Fukuda, Y. Omagari and K. Maruoka, *Angew. Chem. Int. Ed.*, 2015, **54**, 15767-15770.
3. T. Nakamura, K. Okuno, R. Nishiyori and S. Shirakawa, *Chem.-Asian J.*, 2020, **15**, 463-472.
4. O. G. Mancheño and M. Waser, *Eur. J. Org. Chem.*, 2023, **26**, 8.
5. S. Mohapatra, Y. T. Lin, S. G. Goh, C. Ng, L. H. You, N. H. Tran and K. Y. H. Gin, *J. Hazard. Mater.*, 2023, **445**, 130393.
6. M. C. Jennings, K. P. C. Minbiole and W. M. Wuest, *ACS Infect. Dis.*, 2015, **1**, 288-303.
7. D. R. MacFarlane, P. Meakin, J. Sun, N. Amini and M. Forsyth, *J. Phys. Chem. B*, 1999, **103**, 4164-4170.
8. F. Mast, M. M. Hielscher, T. Wirtanen, M. Erichsen, J. Gauss, G. Diezemann and S. R. Waldvogel, *J. Am. Chem. Soc.*, 2024, **146**, 15119-15129.
9. A. E. Somers, B. Khemchandani, P. C. Howlett, J. Z. Sun, D. R. MacFarlane and M. Forsyth, *ACS Appl. Mater. Interfaces*, 2013, **5**, 11544-11553.
10. C. Verma, K. Y. Rhee and M. A. Quraishi, *Adv. Colloid Interface Sci.*, 2022, **306**, 102723.
11. N. M. Mustafa, F. N. Jumaah, N. A. Ludin, M. Akhtaruzzaman, N. H. Hassan, A. Ahmad, K. Chan and M. S. Su'ait, *Heliyon*, 2024, **10**, e27381.
12. P. Gilbert and L. E. Moore, *J. Appl. Microbiol.*, 2005, **99**, 703-715.
13. D. Kwasniewska, Y. L. Chen and D. Wieczorek, *Pathogens*, 2020, **9**, 459.
14. C. C. Zhou and Y. L. Wang, *Curr. Opin. Colloid Interface Sci.*, 2020, **45**, 28-43.
15. S. P. Denyer, *Int. Biodeterior. Biodegrad.*, 1995, **36**, 227-245.
16. A. F. Zahrt, J. J. Henle, B. T. Rose, Y. Wang, W. T. Darrow and S. E. Denmark, *Science*, 2019, **363**, eaau5631.
17. J. J. Henle, A. F. Zahrt, B. T. Rose, W. T. Darrow, Y. Wang and S. E. Denmark, *J. Am. Chem. Soc.*, 2020, **142**, 11578-11592.
18. E. Gousseva, S. D. Midgley, J. M. Seymour, R. Seidel, R. Grau-Crespo and K. R. J. Lovelock, *J. Phys. Chem. B*, 2022, **126**, 10500-10509.
19. E. Gousseva, F. K. Towers Tompkins, J. M. Seymour, L. G. Parker, C. J. Clarke, R. G. Palgrave, R. A. Bennett, R. Grau-Crespo and K. R. J. Lovelock, *J. Phys. Chem. B*, 2024, **128**, 5030-5043.
20. C. H. Suresh and S. Anila, *Acc. Chem. Res.*, 2023, **56**, 1884-1895.
21. S. Men, K. R. J. Lovelock and P. Licence, *Phys. Chem. Chem. Phys.*, 2011, **13**, 15244-15255.
22. R. K. Blundell and P. Licence, *Phys. Chem. Chem. Phys.*, 2014, **16**, 15278-15288.
23. R. K. Blundell and P. Licence, *Chem. Commun.*, 2014, **50**, 12080-12083.
24. R. M. Fogarty, R. G. Palgrave, R. A. Bourne, K. Handrup, I. J. Villar-Garcia, D. J. Payne, P. A. Hunt and K. R. J. Lovelock, *Phys. Chem. Chem. Phys.*, 2019, **21**, 18893-18910.
25. J. M. Seymour, E. Gousseva, A. I. Large, C. J. Clarke, P. Licence, R. M. Fogarty, D. A. Duncan, P. Ferrer, F. Venturini, R. A. Bennett, R. G. Palgrave and K. R. J. Lovelock, *Phys. Chem. Chem. Phys.*, 2021, **23**, 20957-20973.
26. K. R. J. Lovelock, I. J. Villar-Garcia, F. Maier, H. P. Steinrück and P. Licence, *Chem. Rev.*, 2010, **110**, 5158-5190.
27. R. W. Taft, M. Taagepera, J. L. M. Abboud, J. F. Wolf, D. J. Defrees, W. J. Hehre, J. E. Bartmess and R. T. McIver, *J. Am. Chem. Soc.*, 1978, **100**, 7765-7767.
28. L. K. Scarbath-Evers, P. A. Hunt, B. Kirchner, D. R. MacFarlane and S. Zahn, *Phys. Chem. Chem. Phys.*, 2015, **17**, 20205-20216.

View Article Online
DOI: 10.1039/D4CC03388D

Data for this article, including X-ray photoelectron spectroscopy experimental data and log files for all calculated structures will be made available once the article is accepted for publication at University of Reading Research Data Archive. Analysed data supporting this article have been included as part of the Supplementary Information.